Safe Operation of Autonomous Mobile Robots in Human-shared Industrial Workspaces

3D Voronoi tessellation for the study of mechanical behavior of rocks at different scales

A. Insana[1,*] and M. Barla[1]

[1] Department of Structural, Geotechnical and Building Engineering (DISEG), Politecnico di Torino
Corso Duca degli Abruzzi 24, 10129, Torino (Italy)
alessandra.insana@polito.it

Abstract Numerical investigation of crack damage development and micro-fracturing in brittle rocks is a widely studied topic, given the number of applications involved. In the framework of the Discrete Element Method (DEM) formulation, the grain-based distinct element model with random polygonal blocks can represent an alternative to the Bonded-Particle Model (BPM) based on particles. Recently, a new engine called Neper has been made available for generating 3D Voronoi grains. The aim of this study is to investigate the applicability of a Neper-based 3D Voronoi tessellation technique for the simulation of the mechanical macro response of rocks. Simulation of unconfined compression tests on synthetic specimens is conducted and a calibration procedure tested. The issue related to scale effects is also addressed, with an application to the case study of a deep geothermal reservoir.

Keywords: 3D Voronoi tessellation, numerical modelling, Discrete Element Method, grain-based model, upscaling.

1 Introduction

Noticeable advances in brittle failure modelling have taken place in recent years and many approaches have been proposed to this aim. Accounting for fracture mechanisms in rock and rock masses and for damage evolution is crucial for performing realistic simulations both at the laboratory scale and at the field scale (rock slopes, underground excavations). In their reviews, Barla and Beer (2012), Donati et al. (2018) and Lisjak and Grasselli (2014) summarized advantages and shortcomings of some of the most relevant numerical techniques for modelling granular brittle rocks, such as for example the Discrete Element Method (DEM) based on particles (Potyondy and Cundall, 2004) or on Trigon tessellation (Gao and Stead, 2014), the hybrid Finite-Discrete Element Method (FDEM) or the lattice-spring approach. Among the techniques available, Voronoi tessellation has also emerged within the framework of DEM and has been increasingly used to generate a domain discretized in an assembly of random polygonal blocks that can interact with each other through their contact points. This method was widely used thanks to its ability to emulate the grain-based structure of rock-like materials

(Monteiro Azevedo et al., 2014; Farahmand and Diederichs, 2015; Gui et al., 2016). Grain boundaries represent flaws in intact rock and can then act as preferential locations for initiation and propagation of microfractures. However, challenges clearly arise when dealing with numerical methods that try to explicitly simulate the rock structure. Several attempts can be found in literature to find a procedure for microparameters calibration based on the results of uniaxial compression tests, triaxial tests, Brazilian tests and direct tensile tests observed in the laboratory (Kazerani and Zhao, 2010; Insana and Barla, 2017; Li et al., 2017; Ji et al., 2018). Many authors investigated the effect of microparameters on peak and postpeak macroresponse and damage threshold levels, of grains with different size and shape and of pores on fracture patterns, of heterogeneity (grains size distribution) on crack initiation, growth, interaction and ultimate strength.
One of the difficulties in using Voronoi discretization technique is the generation of 3D tessellated domains. Ghazvinian et al. (2014) validated a methodology based on the Neper open-source engine to build the domains against laboratory data on a Cobourg Limestone and managed to capture brittle rock damage and showed its capability to capture rock anisotropy such as grain geometrical alignment.
Still largely unexplored is the definition of proper upscaling rules to describe in situ behavior as more realistically as possible. As claimed by Sinha and Walton (2018), that simulated large underground structures like mine pillars with different slenderness ratios, an impressive laboratory-scale model calibration does not ensure that the modelling approach could be universally acceptable. Moreover, Voronoi model results are strictly dependent on the block size selected (Insana et al., 2016; Sinha and Walton, 2018), which could be different from a laboratory or a field scale numerical model due to computational effort reasons.
In this paper the Discrete Element Method (DEM) with 3D Voronoi tessellation built in Neper is investigated, by focusing on both microparameters calibration at the laboratory scale and upscaling rules. A simple field scale model related to the case study of an Enhanced Geothermal System (EGS) reservoir is also built to test the applicability of the methodology proposed to the simulation of underground rock engineering problems.

2 Laboratory scale

To test the capability of Voronoi tessellation to reproduce the mechanical response of a specimen of intact rock, numerical simulations of unconfined compression tests were performed on a 3D synthetic specimen discretized with Voronoi grains. The initial geometry was created thanks to Neper (Quey et al., 2011), a command-line software for the generation of 2D and 3D polycrystals and meshes. The following steps were followed: i) definition of the domain, a cylinder 0.05 m in diameter and 0.1 m in height, ii) setting of the number of centroids (1000 in this specific case), from which the Voronoi cells are generated, iii) regularization of the tessellation, during which the blocks characterized by the smallest edge of a cell to its average radius ratio lower than a threshold are deleted and the block divided again. This process is particularly useful to avoid the concentration of stresses, by obtaining a better distribution of the equivalent diameter of

grains. The obtained model, shown in Fig. 1a, characterized by an average edge length of 3 mm of the tetrahedric mesh and an equivalent average diameter of 7 mm, was then directly imported in the 3DEC software (Itasca, 2013). The generated polycristals cover the whole domain, with null initial porosity.

To monitor axial strain, axial stress and radial strain during the test, the scheme shown in Fig. 1a was used. Axial strain was referred to sections AA and BB. Each section contains five monitoring points and is located at 10 mm from the specimen top or bottom boundaries. The strain was obtained by averaging the relative displacements of each group of 5 points. Radial strain was computed by averaging the relative displacement of three pairs of points, close to the specimen mid-thickness and 5 mm far from the external boundary (Fig. 1a). Axial stress is the average of that acting in correspondence of the centroids of each zone falling within a parallelepiped of size 40x40x50 mm inside the cylindrical domain. A parametric study allowed to define an appropriate value of velocity applied on the loading plates, that is 0.005 m/s, as in this case the stress-strain behavior could be well reproduced and a good compromise between computational time and results precision was attained.

The properties shown in Table 1 and referred to a Barre granite (Barla, 2010) were assigned to Voronoi blocks, for which an elastic constitutive model was chosen so that cracks can initiate and propagate along the grain edges only.

Table 1 Strength and deformability properties assigned to blocks.

Property	Symbol	Unit	Value
Density	ρ	Kg/m^3	2640
Young's modulus	E	MPa	40000
Poisson's coefficient	υ	-	0.3
Bulk modulus	K	Pa	$3.33 \cdot 10^{10}$
Shear modulus	G	Pa	$1.54 \cdot 10^{10}$
Unconfined compression strength	σ_{ci}	MPa	115.5

The interaction between the contacts of adjacent grains was assigned a plastic model with Coulomb slip failure and residual strength, allowing to simulate joints displacements due to the loss of friction, cohesion and tensile strength at the onset of a tensile or shear fracture. For each contact, initial values of normal and shear stiffness, cohesion, friction angle and tensile strength were defined (Table 2) for the subsequent micro-parameters calibration process. As in Insana et al. (2016), and similarly to a method used also in the Particle Flow Model (Camusso and Barla, 2009) a trial-and-error procedure was followed for this purpose. First, a multiplier S was applied to the stiffness to match the deformability of the material, while keeping constant the strength parameters. Indeed, Ghazvinian at al. (2014), Kazerani and Zhao (2010) and Gao and Stead (2014) demonstrated the direct dependence of the Young's modulus and of the Poisson's coefficient from the contact stiffnesses. Then, the found value of S was kept constant and a multiplier R was modified until a similar value for the laboratory strength was obtained. Values of S=14 and R=1.8 led to a good match of strength and deformability (Fig. 1b).

Table 2 Strength and deformability properties assigned to contacts (from Insana, 2016).

Property	Symbol	Unit	Value
Normal stiffness	k_n	Pa/m	$1.35 \cdot 10^{14}$
Shear stiffness	k_s	Pa/m	$6.73 \cdot 10^{13}$
Cohesion	c	MPa	22.9
Tensile strength	σ_t	MPa	8.9
Friction angle	φ	°	46.9
Residual cohesion	c_{res}	Pa	0
Residual tensile strength	$\sigma_{t,res}$	Pa	0
Residual friction angle	φ_{res}	°	46.9

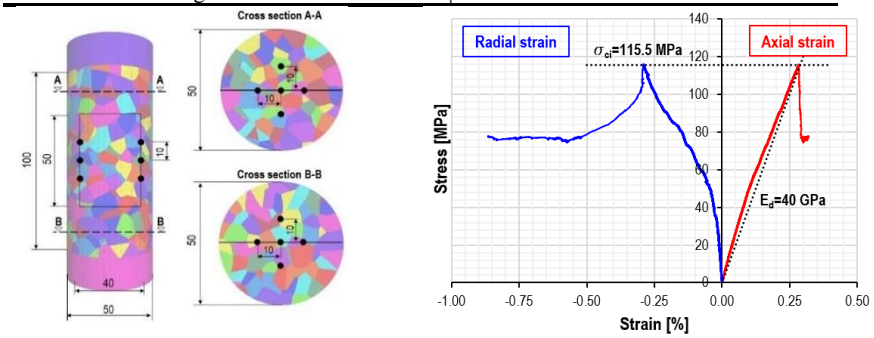

(a) (b)

Fig. 1 (a) Monitoring scheme for calculating the mechanical response of Voronoi tessellated synthetic specimen and (b) calibrated stress-strain curves

3 Scale effects: towards the site scale

While in the previous section an example of microparameters calibration at the laboratory scale was described, in this chapter the effect of scale on strength and deformability will be analyzed. A number of synthetic specimens characterized by the same average edge length of 20 cm (as in the case study described in the following section) and by different size (1x2 m, 2x4 m, 3x6 m, 4x8 m, 5x10 m, 6x12 m where the first number indicates the diameter and the second one is the height) were object of study. All the specimens were assigned the same blocks and joint properties as obtained from section 2 and were tested under unconfined conditions. In this case the calibration refers to the strength properties of the rock mass, shown in Table 3.

The sketch of the numerical models and the results obtained are illustrated in Fig. 2. It can be observed that the smallest specimen presents the highest strength, due to the lower number of grains and, hence, of flaws. Nevertheless, it can also be noticed that, from a size of 3x6 m on, the strength attains a constant value. By assuming that this constant value would be maintained also for the site scale model, calibration was then performed on the 3x6 sample, following the procedure described in section 2.

Satisfactory results able to reproduce the rock mass behavior at a given scale were obtained with S=24 and R=2.2.

Table 3 Rock mass strength properties.

Property	Symbol	Unit	Value
Friction angle	φ	°	34.6
Cohesion	c	MPa	7.3
Tensile strength	σ_t	MPa	0.08
Compressive strength	σ_c	MPa	28.0

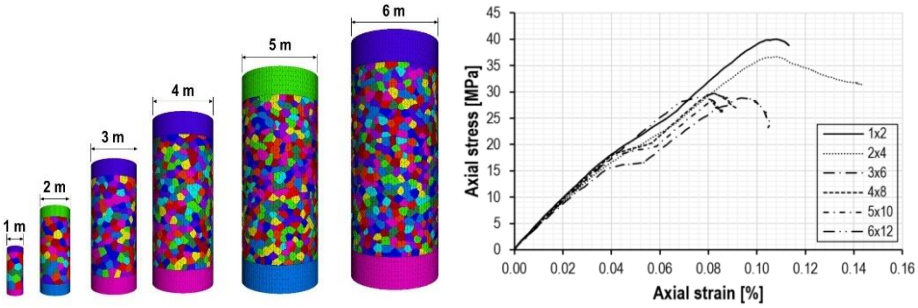

(a) (b)

Fig. 2 Results of unconfined compression tests (b) on synthetic specimens of different sizes (a)

4 Case study

Based on the results obtained in the previous chapters, a simple exercise was performed to test the applicability of Voronoi tessellation for the simulation of a rock engineering problem. The case of a theoretical EGS system was chosen, where high-pressure water is pumped in a well drilled in a hot, deep intact rock mass causing hydraulic fracturing and re-opening of natural joints sealed by the deposition of minerals. This problem has been recently studied by using Voronoi tessellation (Zangeneh et al., 2014; Ghazvinian and Kalenchuk, 2016). The simulation included the drilling of two circular wells, 5 m far and 50 cm in diameter, and hydraulic fracturing of a granitic intact rock mass (Table 3). The domain is limited to 15x10x5 m, as computational time is very critical. Again, the geometry was created in Neper with 12000 grains to obtain an average edge length of 20 cm and then imported in 3DEC. Each grain was then discretized into tetrahedral elements with an edge of 10 cm.

Hydraulic fracturing is supposed to occur at a depth of 4 km. The stress state is considered isotropic and equal to 105.6 MPa. In the present study, the process of hydraulic fracturing was simulated by implementing the HYDRA routine (HYDRaulic fracturing Algorithm, Insana and Barla, 2017) here extended to the 3D case. HYDRA3D identifies the points (subcontacts) of each potential failure surface (contact) and determines in which of these points a fracture is formed. If the subcontact is found to have failed, the

joint is applied a normal pressure that simulates the action of pressurized water. The subsequent effect will be the further opening of the discontinuities. Iteratively, stages of fluid injection and flow along the new surfaces were alternated, until a sufficiently fractured reservoir was obtained. It is pointed out that pressure was applied only in the band between 2 and 3 m in the model to simulate the presence of packers. Pressures applied progressively are shown in Fig. 3.

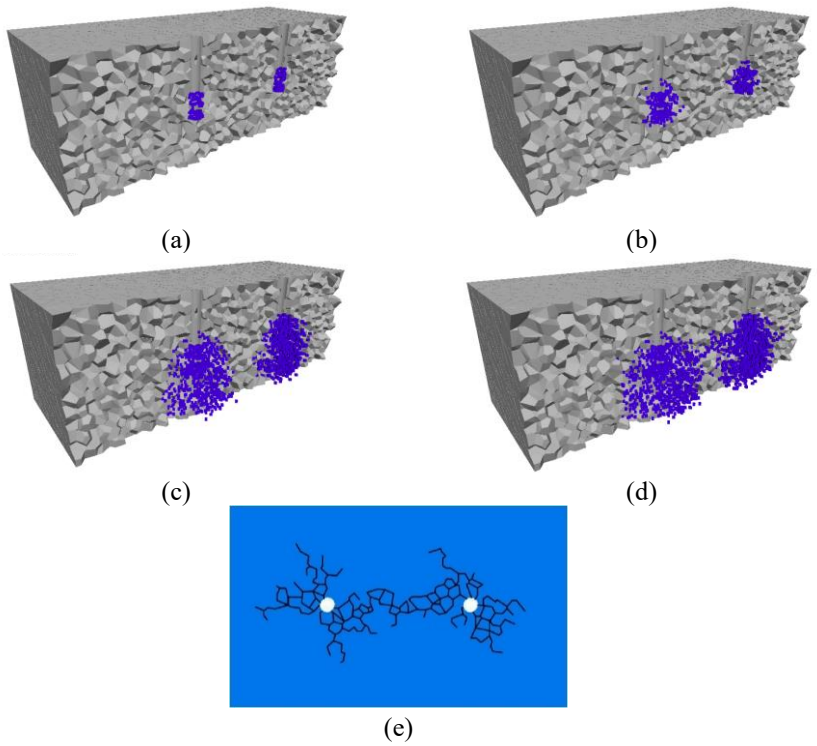

Fig. 3 Pressures applied (a) at the beginning, (b) after 4, (c) 8 and (d) 13 cycles of HYDRA3D and (e) fractures patterns on a mid-thickness cross section at the end of the simulation.

The fractures system at a depth of 2.5 m with a pressure of 300 MPa is represented in Fig. 3e. Most of the contacts are yielded in shear rather than in tension, as in Insana and Barla (2017). Compared to Insana and Barla (2017), it can be seen that the system of fractures propagates in all directions due to the isotropic state of stress. However, the network is much coarser because of the different size in grains, increased in the present study to enhance computational times. The resulting pressure was bigger than in the above-mentioned study, where 250 MPa was obtained, and does not match with common wellhead pressure values which fall typically in the range 10-65 MPa (Zhang and Zhao, 2020). The reason for this overestimation could be attributed to the assumed null initial aperture values at the Voronoi contacts, while for example Zangeneh et al. (2014) distinguish incipient and natural fractures with 0.01 and 0.1 mm initial aperture. Moreover, the rock mass is considered intact, without any preexisting natural joints. Another

aspect to be improved in the modelling is the monotonically increasing pressure applied to the newly formed fractures. Indeed, when injecting, the pressure will not rise indefinitely but a peak pressure is associated to the first fracture nucleation (breakdown pressure) followed by a steady value required to propagate the hydraulic fracture (Guo et al., 2007).

5 Conclusions

The aim of the present work was to show the applicability of Voronoi tessellation generated in Neper for the simulation of fracturing process in rocks, both at the laboratory and at the field scale. The behavior of a synthetic laboratory specimen was reproduced with a distinct element model composed by Voronoi grains by calibrating its microproperties. At the site scale a new calibration was needed, as the size of the grains was modified to 20 cm to keep computational times reasonably short (Insana, 2016). Indeed, a constant size of grains leads to variable strengths and deformabilities when changing the size of the model. However, no significant changes were observed once a certain scale is attained. On this scale microproperties calibration for the site scale model took place. The simulation of hydraulic fracturing involved the use of the bespoke algorithm HYDRA3D, which simulates the propagation of pressurized water and the creation of permeable channels. The scheme of the generated permeable paths is very similar to that obtained in previous studies (Insana et al., 2016; Insana and Barla, 2017). However, the pressure value does not match with typical wellhead pressures (Zhang and Zhao, 2020), showing that the algorithm requires further improvements and comparisons with coupled hydromechanical numerical results (Zangeneh et al., 2014) as well as the rock mass structure needs to be reproduced in a more realistic way.

Acknowledgements The authors are grateful to the students Ilaria Terramagra and Marina Fina for performing the numerical analyses described in the paper.

References

Barla, M. (2010). *Elementi di Meccanica e Ingegneria delle Rocce*. Celid, 320 p.

Barla, M., and Beer, G. (2012). Special issue on Advances in Modeling Rock Engineering problems. Int J Geomech 12(6)

Camusso, M., and Barla, M. (2009). Microparameters calibration for loose and cemented soil when using particle methods. Int J Geomech 9, 217–229

Donati, D., Stead, D., Elmo, D., et al (2018). Experience gained in modelling brittle fracture in rock. In: 52nd U.S. Rock Mechanics/Geomechanics Symposium

Farahmand, K., and Diederichs, M.S. (2015). A calibrated synthetic rock mass (SRM) model for simulating crack growth in granitic rock considering grain scale heterogeneity of

polycrystalline rock. In: 49th US Rock Mechanics / Geomechanics Symposium 2015

Gao, F.Q., and Stead, D. (2014). The application of a modified Voronoi logic to brittle fracture modelling at the laboratory and field scale. Int J Rock Mech Min Sci 68, 1–14

Ghazvinian, E., Diederichs, M.S., and Quey, R. (2014). 3D random Voronoi grain-based models for simulation of brittle rock damage and fabric-guided micro-fracturing. J Rock Mech Geotech Eng 6, 506–521

Ghazvinian, E., and Kalenchuk, K. (2016). Application of 3D random voronoi tessellated models for simulation of hydraulic fracture propagation within the distinct element formulation. In: 50th US Rock Mechanics / Geomechanics Symposium 2016

Gui, Y.L., Zhao, Z.Y., Ji, J., et al (2016). The grain effect of intact rock modelling using discrete element method with voronoi grains. Geotech Lett

Guo, B., Lyons, W.C., and Ghalambor, A. (2007). Petroleum Production Engineering, A Computer-Assisted Approach

Insana, A. (2016). Modeling hydrofracking for deep geothermal energy exploitation by Voronoi tessellation. Politecnico di Torino

Insana, A., and Barla, M. (2017). A Voronoi-based Algorithm for Hydraulic Fracturing Simulation in Deep Geothermal Wells. In: 15th IACMAG, Wuhan, China

Insana, A., Barla, M., and Elmo, D. (2016). Multi Scale Numerical Modelling Related to Hydrofracking for Deep Geothermal Energy Exploitation. Procedia Eng 158, 314–319

Itasca (2013). 3DEC 3 Dimensional Distinct Element Code - User's Guide version 5.0. Minneapolis, MN, USA.

Ji, X., Zhou, W., Chen, Y., and Ma, G. (2018). Generation of the polycrystalline rock microstructure by a novel Voronoi grain-based model with particle growth. In: 52nd U.S. Rock Mechanics/Geomechanics Symposium

Kazerani, T., and Zhao, J. (2010). Micromechanical parameters in bonded particle method for modelling of brittle material failure. Int J Numer Anal Methods Geomech

Li, J., Konietzky, H., and Frühwirt, T. (2017). Voronoi-Based DEM Simulation Approach for Sandstone Considering Grain Structure and Pore Size. Rock Mech Rock Eng 50, 2749–2761

Lisjak, A., and Grasselli, G. (2014). A review of discrete modeling techniques for fracturing processes in discontinuous rock masses. J. Rock Mech. Geotech. Eng.

Monteiro Azevedo, N., Candeias, M., and Gouveia, F. (2014). A Rigid Particle Model for Rock Fracture Following the Voronoi Tessellation of the Grain Structure: Formulation and Validation. Rock Mech Rock Eng 48, 535–557

Potyondy, D.O., and Cundall, P.A. (2004). A bonded-particle model for rock. Int J Rock Mech Min Sci 41, 1329–1364

Quey, R., Dawson, P.R., and Barbe, F. (2011). Large-scale 3D random polycrystals for the finite element method: Generation, meshing and remeshing. Comput Methods Appl Mech Eng

Sinha, S., and Walton, G. (2018). Application of micromechanical modeling to prediction of in-situ rock behavior. In: 52nd U.S. Rock Mechanics/Geomechanics Symposium

Zangeneh, N., Eberhardt, E., and Bustin, R.M. (2014). Investigation of the influence of natural fractures and in situ stress on hydraulic fracture propagation using a distinct-element approach. Can Geotech J

Zhang, Y., and Zhao, G.F. (2020). A global review of deep geothermal energy exploration: from a view of rock mechanics and engineering. Geomech Geophys Geo-Energy Geo-Resources